

A unified formulation for dynamic analysis of nonlocal heterogeneous nanobeams in hygro-thermal environment

Farzad Ebrahimi¹ · Mohammad Reza Barati¹

Received: 20 March 2016 / Accepted: 28 July 2016 / Published online: 6 August 2016
© Springer-Verlag Berlin Heidelberg 2016

Abstract In this article, combined effect of moisture and temperature on free vibration characteristics of functionally graded (FG) nanobeams resting on elastic foundation is investigated by developing various refined beam theories which capture shear deformation influences needless of any shear correction factor. The material properties of FG nanobeam are temperature dependent and change gradually along the thickness through the power-law model. Size-dependent description of the nanobeam is performed applying nonlocal elasticity theory of Eringen. Nonlocal governing equations of embedded FG nanobeam in hygro-thermal environment obtained from Hamilton's principle are solved analytically. To verify the validity of the developed theories, the results of the present work are compared with those available in the literature. The effects of various hygro-thermal loadings, elastic foundation, gradient index, nonlocal parameter, and slenderness ratio on the vibrational behavior of FG nanobeams modeled via various beam theories are explored.

1 Introduction

Hygro-thermal stresses arising from temperature and moisture variations can affect the mechanical performance of engineering structures even at nanoscale. Also, advanced structural components composed of functionally graded materials (FGMs) may experience intense hygro-thermal

environments which show an adverse influence on the stiffness and safety of such structures. Therefore, an accurate evaluation of environmental exposure is necessitated to find the essence of their detrimental influence on the FG structures. Thus, it is of utmost significance to investigate hygro-thermally induced mechanical behavior of these structural elements. To this end, hygro-thermal stress analysis of one-dimensional functionally graded piezoelectric media via analytical solutions is carried out by Akbarzadeh and Chen [1]. Postbuckling of functionally graded (FG) plates under hygro-thermal environments is studied by Lee and Kim [30]. The static behaviors of exponentially inhomogeneous plates subjected to a transverse uniform loading and hygro-thermal conditions are studied by Zenkour [40]. Al Khateeb and Zenkour [4] presented a refined four-variable plate model for bending analysis of advanced plates embedded on elastic foundations in hygro-thermal environments. In another study, Zenkour et al. [41] researched the influence of temperature and moisture on the mechanical behavior of shear-deformable composite FGM plates resting on elastic foundations. Tounsi et al. [36] introduced a refined trigonometric shear deformation theory for thermoelastic bending of FG sandwich plates. Thermomechanical bending response of FGM plates was explored by Hamidi et al. [24] and Boud-erba et al. [10]. Bending analysis of FGM plates under hygro-thermomechanical loading using a four-variable refined plate theory was presented by Zidi et al. [42].

Recently, due to the impotency of classical beam theory or Euler–Bernoulli beam theory (EBT) in adequately modeling of the transverse shear deformations as well as shear correction factor dependency of Timoshenko beam theory (TBT), a number of higher-order theories are proposed and applied in analysis of FG structures. EBT neglects the effects of thickness stretching and shear deformation. This simple theory can be successfully used

✉ Farzad Ebrahimi
febrahimi@eng.ikiu.ac.ir

¹ Department of Mechanical Engineering, Faculty of Engineering, Imam Khomeini International University, Qazvin, Iran

in analysis of slender beams with a large aspect ratio. However, influences of shear and normal deformations may become more considerable for moderately thick beams and plates [6], Helabi et al. [25], and Ait Amar Meziane et al. [3, 7]. Hence, several novel plate theories are suggested accounting for both transverse shear and normal deformations and satisfy the zero traction boundary conditions on the surfaces of the plate without using shear correction factor [9, 11, 31].

Vo et al. [38] provided finite element vibration and buckling analysis of FG sandwich beams through a quasi-3D theory in which both shear deformation and thickness stretching effects are included. Ebrahimi and Salari [12] presented a semi-analytical method for vibrational and buckling analysis of FG nanobeams considering the physical neutral axis position. Recently, Ebrahimi and Barati [16–19] presented static and dynamic modeling of a thermopiezoelectrically actuated nanosize beam subjected to a magnetic field. Most recently small-scale effects on hygro-thermomechanical vibration of temperature-dependent nonhomogeneous nanoscale beams are investigated by Ebrahimi and Barati [20]. Ebrahimi and Barati [21] also proposed a nonlocal higher-order shear deformation beam theory for vibration analysis of size-dependent functionally graded nanobeams.

Due to the characteristic size of beams applied in nanoelectromechanical systems (NEMs), the small-scale impact on their behavior is prominent. It is clear that above-mentioned works cannot predict the small-size impacts on the nanostructures. Thus, the nonlocal elasticity theory suggested by Eringen [22] is developed. He extended the classical continuum mechanics to describe small-scale influences. Based on the nonlocal constitutive relations of Eringen, several studies have been carried out to investigate the mechanical responses of nanostructures. Peddieson et al. [39] indicated that nonlocal continuum mechanics could be applicable to analysis of nanoscale structures. To extend nonlocal elasticity theory for analysis of FG structures, vibrational behavior of nanosize FG beams via finite element method is explored by Eltaher et al. [23]. Tounsi et al. [35, 36] investigated the nonlocal effects on thermal buckling properties of double-walled carbon nanotubes. Size-dependent mechanical behavior of FG trigonometric shear-deformable nanobeams including neutral surface position concept was introduced by Ahouel et al. [2], while Larbi Chaht et al. [29] explored the bending and buckling of FG nanoscale beams including the thickness stretching effect. Also the chirality and scale effects on mechanical buckling properties of zigzag double-walled carbon nanotubes were investigated by Benguediab et al. [8].

The influences of various thermal environments on buckling and vibration of nonlocal temperature-dependent FG beams are analyzed by Ebrahimi and Salari [14] using Navier analytical solution. In another work, Ebrahimi and

Salari [13] investigated thermomechanical vibration of FG nanobeams with arbitrary boundary conditions applying differential transform method (DTM). Also, Ebrahimi et al. [15] explored the effects of linear and nonlinear temperature distributions on vibration of FG nanobeams.

Hygro-thermal analysis of nanostructures is reported in a few works. Small-scale bending analysis of nanoplates resting on elastic foundation under hygro-thermomechanical environments is performed by Alzahrani et al. [5]. Also, using trigonometric shear deformation plate theory, Sobhy [34] investigated vibrational behavior of orthotropic double-layered graphene sheets subjected to hygro-thermal loading. Therefore, it is evident that there is no published work studying hygro-thermomechanical vibration analysis of FG nanobeams with or without elastic foundation using higher-order shear deformation theories.

In this study, a unified higher-order beam theory containing parabolic, sinusoidal, hyperbolic, exponential, and inverse cotangential functions is developed to investigate the influences of moisture and temperature rise due to various hygro-thermal loads on small-amplitude vibration of nanosize FGM beams resting on elastic foundation. These theories provide a constant transverse displacement and higher-order variation of axial displacement through the depth of the nanobeam so that there is no need for any shear correction factors. Three types of environmental condition namely uniform, linear, and sinusoidal hygro-thermal loading are studied. The material properties of FGM nanobeam are regarded to be temperature dependent and are graded in the thickness direction via power-law model. An analytical solution is applied to solve the governing equations derived from Hamilton's principle. Several numerical and illustrative results are presented to indicate the effects of the shear deformation, various hygro-thermal environments, gradient index, nonlocality, and elastic foundation parameters on the hygro-thermomechanical vibration of FG nanobeams.

2 Theory and formulation

2.1 Power-law FG nanobeam model

A FG nanobeam system of length a , width b , and thickness h is shown in Fig. 1. The effective material properties of the nonlocal FG beam including Young's modulus E_f , moisture expansion coefficient β_f , thermal expansion α_f , and mass density ρ_f change continuously in the z -axis direction (thickness direction) according to power-law model. Hence, the effective material properties, P_f , can be stated as:

$$P_f = P_c V_c + P_m V_m \quad (1)$$

Fig. 1 Geometry of functionally graded nanobeam resting on elastic foundation

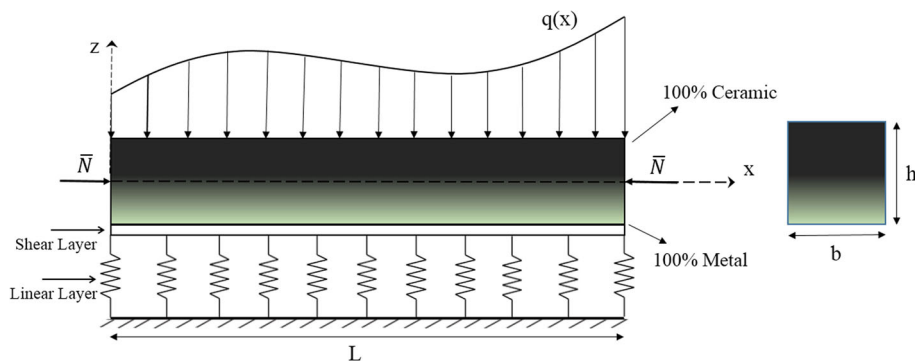


Table 1 Shape functions

Beam theory	$f(z)$
Parabolic (PSDT [33])	$\frac{4z^3}{3h^2}$
Sinusoidal (TSDT [37])	$z - \frac{h}{\pi} \sin\left(\frac{\pi z}{h}\right)$
Exponential (ESDT [26])	$z - ze^{-2\left(\frac{z}{h}\right)^2}$
Hyperbolic (HSDT [27])	$z - z\left[1 + \frac{3\pi}{2} \operatorname{sech}^2\left(\frac{1}{2}\right)\right] + \frac{3\pi}{2} h \tanh\left(\frac{z}{h}\right)$
Inverse cotangential (ITSDT [28])	$z - \cot^{-1}\left(\frac{rh}{z}\right) + \frac{4r}{h(4r^2+1)}$; $r = 0.46$

In which $P_m, P_c, V_m,$ and V_c denote the metal and ceramic material properties and its volume fractions which have a relation with the following form:

$$V_c + V_m = 1 \tag{2}$$

The ceramic phase volume fraction of the nanobeam is described as:

$$V_c = \left(\frac{z}{h} + \frac{1}{2}\right)^p \tag{3}$$

Here p is the power-law index which is a nonnegative variable and estimates the material distribution through the nanobeam thickness, and z is the distance from the mid-surface of the nanobeam. It is clear that when p is equal to zero, the FG nanobeam is fully ceramic. So, according to Eqs. (1)–(2), the effective material properties of the non-local FGM beam including Young’s modulus (E), mass density (ρ), thermal expansion (α), and moisture expansion coefficient (β) can be expressed in the following form:

$$\begin{aligned} E(z) &= (E_c - E_m)\left(\frac{z}{h} + \frac{1}{2}\right)^p + E_m \\ \rho(z) &= (\rho_c - \rho_m)\left(\frac{z}{h} + \frac{1}{2}\right)^p + \rho_m \\ \alpha(z) &= (\alpha_c - \alpha_m)\left(\frac{z}{h} + \frac{1}{2}\right)^p + \alpha_m \\ \beta(z) &= (\beta_c - \beta_m)\left(\frac{z}{h} + \frac{1}{2}\right)^p + \beta_m \end{aligned} \tag{4}$$

For more precise anticipation of FGMs behavior under extreme temperature fields, material properties must be

dependent on temperature. Therefore, temperature-dependent coefficients of material phases can be expressed according to the following nonlinear equation:

$$P = P_0(P_{-1} T^{-1} + 1 + P_1 T + P_2 T^2 + P_3 T^3) \tag{5}$$

where P_0, P_{-1}, P_1, P_2 and P_3 are the temperature-dependent coefficients which are tabulated in Table 2 for Si_3N_4 and SUS 304. The bottom and top surfaces of FG nanobeam are supposed to be fully metal (SUS 304) and fully ceramic (Si_3N_4), respectively.

2.2 Kinematic relations

Based on the refined shear deformation beam theories, the displacement field at any point of the beam can be written as:

$$u_x(x, z) = u(x) - z \frac{\partial w_b}{\partial x} - f(z) \frac{\partial w_s}{\partial x} \tag{6}$$

$$u_z(x, z) = w_b(x) + w_s(x) \tag{7}$$

where u is longitudinal displacement and w_b, w_s are the bending and shear components of transverse displacement of a point on the midplane of the beam. $f(z)$ is the shape function determining the distribution of the transverse shear strain and shear stress through the thickness of the beam for which various beam models (parabolic, sinusoidal, hyperbolic, exponential and inverse cotangential) are presented in Table 1. Nonzero strains of the present beam model are expressed as follows:

$$\varepsilon_{xx} = \frac{\partial u}{\partial x} - z \frac{\partial^2 w_b}{\partial x^2} - f(z) \frac{\partial^2 w_s}{\partial x^2} \tag{8}$$

$$\gamma_{xz} = g \frac{\partial w_s}{\partial x} \tag{9}$$

where $g(z) = 1 - df/dz$. By using the Hamilton’s principle, in which the motion of an elastic structure in the time interval $t1 < t < t2$ is so that the integral with respect to time of the total potential energy is extremum:

$$\int_0^t \delta(U + V - K) dt = 0 \tag{10}$$

Here U is strain energy, V is work done by external forces, and K is kinetic energy. The virtual strain energy can be written as:

$$\delta U = \int_v \sigma_{ij} \delta \epsilon_{ij} dV = \int_v (\sigma_{xx} \delta \epsilon_{xx} + \sigma_{xz} \delta \gamma_{xz}) dV \tag{11}$$

Substituting Eqs. (8)–(9) into Eq. (11) yields:

$$\delta U = \int_0^L \left(N \frac{d\delta u}{dx} - M_b \frac{d^2 \delta w_b}{dx^2} - M_s \frac{d^2 \delta w_s}{dx^2} + Q \frac{d\delta w_s}{dx} \right) dx \tag{12}$$

In which the variables introduced in arriving at the last expression are defined as follows:

$$N = \int_A \sigma_{xx} dA, M_b = \int_A z \sigma_{xx} dA, M_s = \int_A f \sigma_{xx} dA, Q = \int_A g \sigma_{xz} dA \tag{13}$$

The first variation of the work done by applied forces can be written in the form:

$$\delta V = \int_0^L \left((N^T + N^H) \left(\frac{d(w_b + w_s)}{dx} \frac{d\delta(w_b + w_s)}{dx} \right) - k_w \delta(w_b + w_s) + k_p \left(\frac{d^2(w_b + w_s)}{dx^2} + \frac{d^2\delta(w_b + w_s)}{dx^2} \right) \right) dx \tag{14}$$

where k_w and k_p are linear and shear coefficient of elastic foundation, respectively, and N^T and N^H are applied forces due to temperature and moisture change as:

$$N^T = \int_{-h/2}^{h/2} E(z, T) \alpha(z, T) (T - T_0) dz, N^H = \int_{-h/2}^{h/2} E(z, T) \beta(z, T) (C - C_0) dz \tag{15}$$

where T_0 and C_0 are the reference temperature and moisture concentrations, respectively. The variation of the kinetic energy can be expressed as:

$$\delta K = \int_0^L \left(I_0 \left[\frac{du}{dt} \frac{d\delta u}{dt} + \left(\frac{dw_b}{dt} + \frac{dw_s}{dt} \right) \left(\frac{d\delta w_b}{dt} + \frac{d\delta w_s}{dt} \right) \right] - I_1 \left(\frac{du}{dt} \frac{d^2 \delta w_b}{dx dt} + \frac{d^2 w_b}{dx dt} \frac{d\delta u}{dt} \right) + I_2 \left(\frac{d^2 w_b}{dx dt} \frac{d^2 \delta w_b}{dx dt} \right) - J_1 \left(\frac{du}{dt} \frac{d^2 \delta w_s}{dx dt} + \frac{d^2 w_s}{dx dt} \frac{d\delta u}{dt} \right) + K_2 \left(\frac{d^2 w_s}{dx dt} \frac{d^2 \delta w_s}{dx dt} \right) + J_2 \left(\frac{d^2 w_b}{dx dt} \frac{d^2 \delta w_s}{dx dt} + \frac{d^2 w_s}{dx dt} \frac{d^2 \delta w_b}{dx dt} \right) \right) dx \tag{16}$$

where

$$(I_0, I_1, J_1, I_2, J_2, K_2) = \int_A \rho(z) (1, z, f, z^2, zf, f^2) dA \tag{17}$$

The following Euler–Lagrange equations are obtained by inserting Eqs. (12)–(16) in Eq. (10) when the coefficients of δu , δw_b and δw_s are equal to zero:

$$\frac{\partial N}{\partial x} = I_0 \frac{d^2 u}{dt^2} - I_1 \frac{d^3 w_b}{dx dt^2} - J_1 \frac{d^3 w_s}{dx dt^2} \tag{18}$$

$$\frac{d^2 M_b}{dx^2} = (N^T + N^H) \frac{d^2(w_b + w_s)}{dx^2} + I_0 \left(\frac{d^2 w_b}{dt^2} + \frac{d^2 w_s}{dt^2} \right) + I_1 \frac{d^3 u}{dx dt^2} - I_2 \frac{d^4 w_b}{dx^2 dt^2} - J_2 \frac{d^4 w_s}{dx^2 dt^2} + k_w (w_b + w_s) - k_p \frac{d^2(w_b + w_s)}{dx^2} \tag{19}$$

$$\frac{d^2 M_s}{dx^2} + \frac{dQ}{dx} = (N^T + N^H) \frac{d^2(w_b + w_s)}{dx^2} + I_0 \left(\frac{d^2 w_b}{dt^2} + \frac{d^2 w_s}{dt^2} \right) + J_1 \frac{d^3 u}{dx dt^2} - J_2 \frac{d^4 w_b}{dx^2 dt^2} - K_2 \frac{d^4 w_s}{dx^2 dt^2} + k_w (w_b + w_s) - k_p \frac{d^2(w_b + w_s)}{dx^2} \tag{20}$$

2.3 The nonlocal elasticity model for FG nanobeam

According to Eringen nonlocal elasticity model [22] which contains wide-range interactions between points in a continuum solid, the stress state at a point inside a body is regarded to be function of all neighbor points’ strains. Hence, in the present work in order to capture the small-size impacts, nonlocal elasticity theory is implemented in which a linear differential framework of constitutive equations is expressed as:

$$(1 - (e_0 a) \nabla^2) \sigma_{kl} = t_{kl} \tag{21}$$

In which ∇^2 denotes the Laplacian operator. Therefore, the scale length $e_0 a$ considers the influences of small size on the

response of nanoscale structures. Thus, the constitutive relations of nonlocal theory for a FG nanobeam can be stated as:

$$\sigma_{xx} - \mu \frac{\partial^2 \sigma_{xx}}{\partial x^2} = E(z)\epsilon_{xx} \tag{22}$$

$$\sigma_{xz} - \mu \frac{\partial^2 \sigma_{xz}}{\partial x^2} = G(z)\gamma_{xz} \tag{23}$$

where $(\mu = (e_0a)^2)$. By integrating Eqs. (22) and (23) over the area of nanobeam's cross section, the following relations for a nonlocal refined FG beam model can be obtained:

$$N - \mu \frac{d^2 N}{dx^2} = A \frac{du}{dx} - B \frac{d^2 w_b}{dx^2} - B_s \frac{d^2 w_s}{dx^2} \tag{24}$$

$$M_b - \mu \frac{d^2 M_b}{dx^2} = B \frac{du}{dx} - D \frac{d^2 w_b}{dx^2} - D_s \frac{d^2 w_s}{dx^2} \tag{25}$$

$$M_s - \mu \frac{d^2 M_s}{dx^2} = B_s \frac{du}{dx} - D_s \frac{d^2 w_b}{dx^2} - H_s \frac{d^2 w_s}{dx^2} \tag{26}$$

$$Q - \mu \frac{d^2 Q}{dx^2} = A_s \frac{dw_s}{dx} \tag{27}$$

where the cross-sectional rigidities are calculated as follows:

$$(A, B, B_s, D, D_s, H_s) = \int_A E(z) (1, z, f, z^2, zf, f^2) dA \tag{28}$$

$$A_s = \int_A g^2 G(z) dA \tag{29}$$

The nonlocal governing equations of refined shear-deformable FG nanobeams in terms of the displacement can be obtained by inserting $N, M_b, M_s,$ and Q from Eqs. (24)–(27), respectively, into Eqs. (18)–(20) as follows:

$$A \frac{d^2 u}{dx^2} - B \frac{\partial^3 w_b}{\partial x^3} - B_s \frac{\partial^3 w_s}{\partial x^3} - I_0 \frac{d^2 u}{dt^2} + I_1 \frac{d^3 w_b}{dx dt^2} + J_1 \frac{d^3 w_s}{dx dt^2} + \mu \left(I_0 \frac{d^4 u}{dx^2 dt^2} - I_1 \frac{d^5 w_b}{dx^3 dt^2} - J_1 \frac{d^5 w_s}{dx^3 dt^2} \right) = 0 \tag{30}$$

$$B \frac{d^3 u}{dx^3} - D \frac{d^4 w_b}{dx^4} - D_s \frac{d^4 w_s}{dx^4} - (N^T + N^H) \frac{d^2(w_b + w_s)}{dx^2} - I_0 \left(\frac{d^2 w_b}{dt^2} + \frac{d^2 w_s}{dt^2} \right) - I_1 \frac{d^3 u}{dx dt^2} + I_2 \frac{d^4 w_b}{dx^2 dt^2} + J_2 \frac{d^4 w_s}{dx^2 dt^2} - k_w(w_b + w_s) + k_p \frac{d^2(w_b + w_s)}{dx^2} + \mu \left((N^T + N^H) \frac{d^4(w_b + w_s)}{dx^4} + I_0 \left(\frac{d^4 w_b}{dx^2 dt^2} + \frac{d^4 w_s}{dx^2 dt^2} \right) + I_1 \frac{d^5 u}{dx^3 dt^2} - I_2 \frac{d^6 w_b}{dx^4 dt^2} - J_2 \frac{d^6 w_s}{dx^4 dt^2} + k_w \frac{d^2(w_b + w_s)}{dx^2} - k_p \frac{d^4(w_b + w_s)}{dx^4} \right) = 0 \tag{31}$$

$$B_s \frac{d^3 u}{dx^3} - D_s \frac{d^4 w_b}{dx^4} - H_s \frac{d^4 w_s}{dx^4} + A_s \frac{d^2 w_s}{dx^2} - (N^T + N^H) \frac{d^2(w_b + w_s)}{dx^2} - I_0 \left(\frac{d^2 w_b}{dt^2} + \frac{d^2 w_s}{dt^2} \right) - J_1 \frac{d^3 u}{dx dt^2}$$

$$+ J_2 \frac{d^4 w_b}{dx^2 dt^2} + K_2 \frac{d^4 w_s}{dx^2 dt^2} - k_w(w_b + w_s) + k_p \frac{d^2(w_b + w_s)}{dx^2} + \mu \left((N^T + N^H) \frac{d^4(w_b + w_s)}{dx^4} + I_0 \left(\frac{d^4 w_b}{dx^2 dt^2} + \frac{d^4 w_s}{dx^2 dt^2} \right) + J_1 \frac{d^5 u}{dx^3 dt^2} - J_2 \frac{d^6 w_b}{dx^4 dt^2} - K_2 \frac{d^6 w_s}{dx^4 dt^2} + k_w \frac{d^2(w_b + w_s)}{dx^2} - k_p \frac{d^4(w_b + w_s)}{dx^4} \right) = 0 \tag{32}$$

3 Solution procedures

Here, to satisfy simply supported boundary condition for hygro-thermomechanical free vibration of FG nanobeams, analytical solution of the coupled governing equations is proposed. To this purpose, the displacement variables adopted are of the form:

$$u(x, t) = \sum_{n=1}^{\infty} U_n \cos(\alpha x) e^{i\omega_n t} \tag{33}$$

$$w_b(x, t) = \sum_{n=1}^{\infty} W_{bn} \sin(\alpha x) e^{i\omega_n t} \tag{34}$$

$$w_s(x, t) = \sum_{n=1}^{\infty} W_{sn} \sin(\alpha x) e^{i\omega_n t} \tag{35}$$

where $\alpha = \frac{n\pi}{L}$ and (U_n, W_{bn}, W_{sn}) are the unknown Fourier coefficients. Inserting Eqs. (33)–(35) into Eqs. (30)–(32), respectively, leads to:

$$\left\{ \left(\begin{matrix} k_{11} & k_{12} & k_{13} \\ k_{21} & k_{22} & k_{23} \\ k_{31} & k_{32} & k_{33} \end{matrix} \right) - \bar{\omega}_n^2 \left(\begin{matrix} m_{11} & m_{12} & m_{13} \\ m_{21} & m_{22} & m_{23} \\ m_{31} & m_{32} & m_{33} \end{matrix} \right) \right\} \left\{ \begin{matrix} U_n \\ W_{bn} \\ W_{sn} \end{matrix} \right\} = 0 \tag{36}$$

where

$$\begin{aligned} k_{1,1} &= -A\alpha^2, & k_{1,2} &= B\alpha^3, & k_{1,3} &= B_s\alpha^3, & k_{2,3} &= -D_s\alpha^4, \\ k_{2,2} &= (N^T + N^H)\alpha^2(1 + \mu\alpha^2) - k_p\alpha^2(1 + \mu\alpha^2) - k_w(1 + \mu\alpha^2) - D\alpha^4, \\ k_{3,3} &= (N^T + N^H)\alpha^2(1 + \mu\alpha^2) - k_p\alpha^2(1 + \mu\alpha^2) - k_w(1 + \mu\alpha^2) - A_s\alpha^2 - H_s\alpha^4, \\ m_{1,1} &= I_0(1 + \mu\alpha^2), & m_{1,2} &= -I_1\alpha - \mu I_1\alpha^3, \\ m_{1,3} &= -J_1\alpha - \mu J_1\alpha^3, \\ m_{2,2} &= I_0(1 + \mu\alpha^2) + I_2\alpha^2 + \mu I_2\alpha^4, \\ m_{2,3} &= I_0(1 + \mu\alpha^2) + J_2\alpha^2 + \mu J_2\alpha^4; \\ m_{3,3} &= I_0(1 + \mu\alpha^2) + K_2\alpha^2 + \mu K_2\alpha^4, \end{aligned} \tag{37}$$

Table 2 Temperature-dependent material properties of FGM constituents [13]

Material	Properties	P_0	P_{-1}	P_1	P_2	P_3
Si ₃ N ₄	E (Pa)	348.43e+9	0	-3.070 e-4	2.160e-7	-8.946
	α (K ⁻¹)	5.8723e-6	0	9.095e-4	0	0
	ρ (kg/m ³)	2370	0	0	0	0
	ν	0.24	0	0	0	0
SUS 304	E (Pa)	201.04e+9	0	3.079e-4	-6.534e-7	0
	α (K ⁻¹)	12.330e-6	0	8.086e-4	0	0
	ρ (kg/m ³)	8166	0	0	0	0
	ν	0.3262	0	-2.002e-4	3.797e-7	0

Table 3 Comparison of the nondimensional frequency of a FG nanobeam under linear temperature rise without elastic foundation ($L/h = 20$)

μ (nm ²)	$p = 0$		$p = 0.2$		$p = 1$		$p = 5$	
	TBT [15]	Present	TBT [13]	Present	TBT [13]	Present	TBT [13]	Present
0	9.1475	9.15733	7.342	7.34189	5.3537	5.34002	4.2875	4.26591
1	8.6601	8.67039	6.9419	6.94219	5.048	5.03448	4.0317	4.00998
2	8.231	8.24169	6.5892	6.58979	4.7777	4.76429	3.8049	3.78297
3	7.8488	7.85997	6.2747	6.27558	4.536	4.5226	3.6015	3.57925
4	7.5053	7.51682	5.9916	5.99269	4.3177	4.30429	3.4172	3.3946

Table 4 Variation of the fundamental nondimensional frequencies of S-S FG nanobeam under uniform hygro-thermal loading for various beam theories ($K_w = K_p = 0, L/h = 20$)

μ	Beam theory	$(\Delta T, \Delta C) = (0, 0)$			$(\Delta T, \Delta C) = (1, 20)$			$(\Delta T, \Delta C) = (2, 40)$		
		$p = 0.2$	$p = 1$	$p = 5$	$p = 0.2$	$p = 1$	$p = 5$	$p = 0.2$	$p = 1$	$p = 5$
0	CBT	7.97186	5.93447	4.84828	7.44767	5.22017	4.01029	6.87174	4.37638	2.92354
	PSDBT	7.96802	5.93142	4.84498	7.44355	5.21668	4.00630	6.86728	4.37221	2.91804
	TSDBT	7.96806	5.93144	4.84498	7.44359	5.21671	4.00630	6.86732	4.37224	2.91804
	ESDBT	7.96817	5.93152	4.84503	7.44371	5.2168	4.00636	6.86745	4.37235	2.91813
	HSDBT	7.96804	5.93143	4.84497	7.44357	5.21669	4.00629	6.8673	4.37223	2.91803
	ITSDBT	7.96847	5.93175	4.84522	7.44404	5.21707	4.00659	6.86781	4.37267	2.91844
1	CBT	7.60538	5.66165	4.62539	7.05386	4.90744	3.73731	6.4427	3.99785	2.53565
	PSDBT	7.60172	5.65874	4.62224	7.0499	4.90406	3.73341	6.43837	3.9937	2.52988
	TSDBT	7.60175	5.65876	4.62224	7.04994	4.90409	3.73341	6.43841	3.99373	2.52988
	ESDBT	7.60186	5.65884	4.62229	7.05005	4.90418	3.73347	6.43853	3.99384	2.52998
	HSDBT	7.60174	5.65875	4.62224	7.04992	4.90408	3.7334	6.43839	3.99372	2.52987
	ITSDBT	7.60215	5.65906	4.62247	7.05037	4.90444	3.73369	6.43888	3.99416	2.5303
2	CBT	7.2852	5.4233	4.43067	6.70727	4.63011	3.49302	6.06116	3.65178	2.15895
	PSDBT	7.28169	5.42051	4.42765	6.70345	4.62682	3.48919	6.05693	3.64761	2.15273
	TSDBT	7.28173	5.42053	4.42765	6.70349	4.62685	3.48919	6.05697	3.64764	2.15273
	ESDBT	7.28183	5.42061	4.4277	6.7036	4.62694	3.48925	6.0571	3.64776	2.15283
	HSDBT	7.28171	5.42052	4.42765	6.70347	4.62684	3.48918	6.05695	3.64763	2.15272
	ITSDBT	7.28211	5.42082	4.42787	6.7039	4.62719	3.48947	6.05743	3.64807	2.15318

Table 5 Variation of the fundamental nondimensional frequencies of S–S FG nanobeam under linear hygro-thermal loading for various beam theories ($K_w = K_p = 0, L/h = 20$)

μ	Beam theory	$(\Delta T, \Delta C) = (0, 0)$			$(\Delta T, \Delta C) = (1, 20)$			$(\Delta T, \Delta C) = (2, 40)$		
		$p = 0.2$	$p = 1$	$p = 5$	$p = 0.2$	$p = 1$	$p = 5$	$p = 0.2$	$p = 1$	$p = 5$
0	CBT	7.88513	5.85175	4.76926	7.66750	5.56297	4.39707	7.43796	5.25198	3.98250
	PSDBT	7.88167	5.84907	4.7664	7.66493	5.56148	4.39598	7.43625	5.25156	3.98286
	TSDBT	7.88174	5.84913	4.76645	7.66510	5.56166	4.3962	7.4365	5.25185	3.98320
	ESDBT	7.88189	5.84926	4.76655	7.66534	5.56191	4.39647	7.43684	5.25219	3.98358
	HSDBT	7.88171	5.8491	4.76642	7.66501	5.56157	4.39609	7.43638	5.25171	3.98304
	ITSDBT	7.88083	5.84813	4.76526	7.66093	5.5563	4.38879	7.42907	5.24214	3.96966
1	CBT	7.51438	5.5748	4.5424	7.28554	5.27052	4.14947	7.04344	4.94085	3.70687
	PSDBT	7.51111	5.57227	4.53971	7.2832	5.26924	4.14862	7.04198	4.94067	3.70747
	TSDBT	7.51119	5.57234	4.53976	7.28337	5.26943	4.14884	7.04225	4.94096	3.7078
	ESDBT	7.51134	5.57246	4.53986	7.28362	5.26968	4.14912	7.04258	4.94131	3.70818
	HSDBT	7.51115	5.57231	4.53973	7.28329	5.26934	4.14873	7.04212	4.94082	3.70764
	ITSDBT	7.51019	5.57126	4.53849	7.27897	5.26378	4.14107	7.03442	4.93078	3.69361
2	CBT	7.19012	5.33249	4.34386	6.95047	5.01323	3.93075	6.69615	4.66513	3.45986
	PSDBT	7.18702	5.3301	4.34133	6.94834	5.01212	3.93010	6.69493	4.66515	3.46065
	TSDBT	7.1871	5.33017	4.34138	6.94852	5.01232	3.93033	6.6952	4.66544	3.46099
	ESDBT	7.18724	5.33029	4.34148	6.94877	5.01257	3.93061	6.69554	4.66579	3.46135
	HSDBT	7.18706	5.33014	4.34135	6.94843	5.01223	3.93022	6.69507	4.6653	3.46083
	ITSDBT	7.18602	5.32902	4.34004	6.9439	5.00641	3.92221	6.68702	4.65481	3.44618

Table 6 Variation of the fundamental nondimensional frequencies of S–S FG nanobeam under sinusoidal hygro-thermal loading for various beam theories ($K_w = K_p = 0, L/h = 20$)

μ	Beam theory	$(\Delta T, \Delta C) = (0, 0)$			$(\Delta T, \Delta C) = (1, 20)$			$(\Delta T, \Delta C) = (2, 40)$		
		$p = 0.2$	$p = 1$	$p = 5$	$p = 0.2$	$p = 1$	$p = 5$	$p = 0.2$	$p = 1$	$p = 5$
0	CBT	7.88513	5.85175	4.76926	7.7383	5.66427	4.51641	7.58466	5.4659	4.24321
	PSDBT	7.88167	5.84907	4.7664	7.73545	5.66239	4.5148	7.58241	5.46477	4.24272
	TSDBT	7.88174	5.84913	4.76645	7.73559	5.66254	4.51498	7.58261	5.465	4.24299
	ESDBT	7.88189	5.84926	4.76655	7.73581	5.66274	4.5152	7.58289	5.46528	4.24332
	HSDBT	7.88171	5.8491	4.76642	7.73552	5.66246	4.51489	7.58251	5.46489	4.24286
	ITSDBT	7.88083	5.84813	4.76526	7.73246	5.65865	4.50946	7.57724	5.45822	4.2332
1	CBT	7.51438	5.5748	4.5424	7.36002	5.37735	4.27575	7.1982	5.16772	3.98573
	PSDBT	7.51111	5.57227	4.53971	7.35739	5.37566	4.27436	7.19619	5.16681	3.98549
	TSDBT	7.51119	5.57234	4.53976	7.35753	5.37581	4.27454	7.1964	5.16703	3.98577
	ESDBT	7.51134	5.57246	4.53986	7.35775	5.37602	4.27477	7.19668	5.16732	3.98609
	HSDBT	7.51115	5.57231	4.53973	7.35746	5.37574	4.27445	7.1963	5.16692	3.98563
	ITSDBT	7.51019	5.57126	4.53849	7.35422	5.37171	4.26875	7.19074	5.15991	3.9755
2	CBT	7.19012	5.33249	4.34386	7.02851	5.12543	4.06385	6.85877	4.90481	3.75718
	PSDBT	7.18702	5.3301	4.34133	7.02608	5.12391	4.06266	6.85698	4.90409	3.75715
	TSDBT	7.1871	5.33017	4.34138	7.02623	5.12407	4.06285	6.8572	4.90432	3.75744
	ESDBT	7.18724	5.33029	4.34148	7.02644	5.12428	4.06308	6.85748	4.90461	3.75777
	HSDBT	7.18706	5.33014	4.34135	7.02615	5.12399	4.06276	6.85709	4.90421	3.7573
	ITSDBT	7.18602	5.32902	4.34004	7.02273	5.11977	4.05679	6.85126	4.89687	3.74672

4 Various hygro-thermal environments

4.1 Uniform moisture and temperature rise

For a FG nanobeam at reference moisture concentration C_0 and reference temperature T_0 , the moisture and temperature are uniformly raised to a final value C and T , respectively, in which the moisture and temperature change are $\Delta T = T - T_0$ and $\Delta C = C - C_0$.

4.2 Linear moisture and temperature rise

For a FG nanobeam for which the plate thickness is thin enough, the moisture and temperature distributions are linearly variable through the thickness as follows:

$$T = T_m + (\Delta T) \left(\frac{1}{2} + \frac{z}{h} \right), \quad C = C_m + (\Delta C) \left(\frac{1}{2} + \frac{z}{h} \right) \quad (38)$$

The $(\Delta T, \Delta C)$ in Eq. (38) could be defined $\Delta T = T_c - T_m$, $\Delta C = C_c - C_m$.

4.3 Sinusoidal moisture and temperature rise

The moisture and temperature fields when FG nanobeam is exposed to sinusoidal moisture/temperature rise across the thickness can be defined as [32]:

$$\begin{aligned} T &= T_m + \Delta T \left(1 - \cos \frac{\pi}{2} \left(\frac{1}{2} + \frac{z}{h} \right) \right), \\ C &= C_m + \Delta C \left(1 - \cos \frac{\pi}{2} \left(\frac{1}{2} + \frac{z}{h} \right) \right) \end{aligned} \quad (39)$$

where $\Delta T = T_c - T_m$ and $\Delta C = C_c - C_m$ are temperature and moisture change.

5 Numerical results and discussion

The results of various numerical analyses are provided in this section for hygro-thermomechanical vibration analysis of a simply supported nanoscale FGM beam modeled via various higher-order shear deformation theories (PSDT,

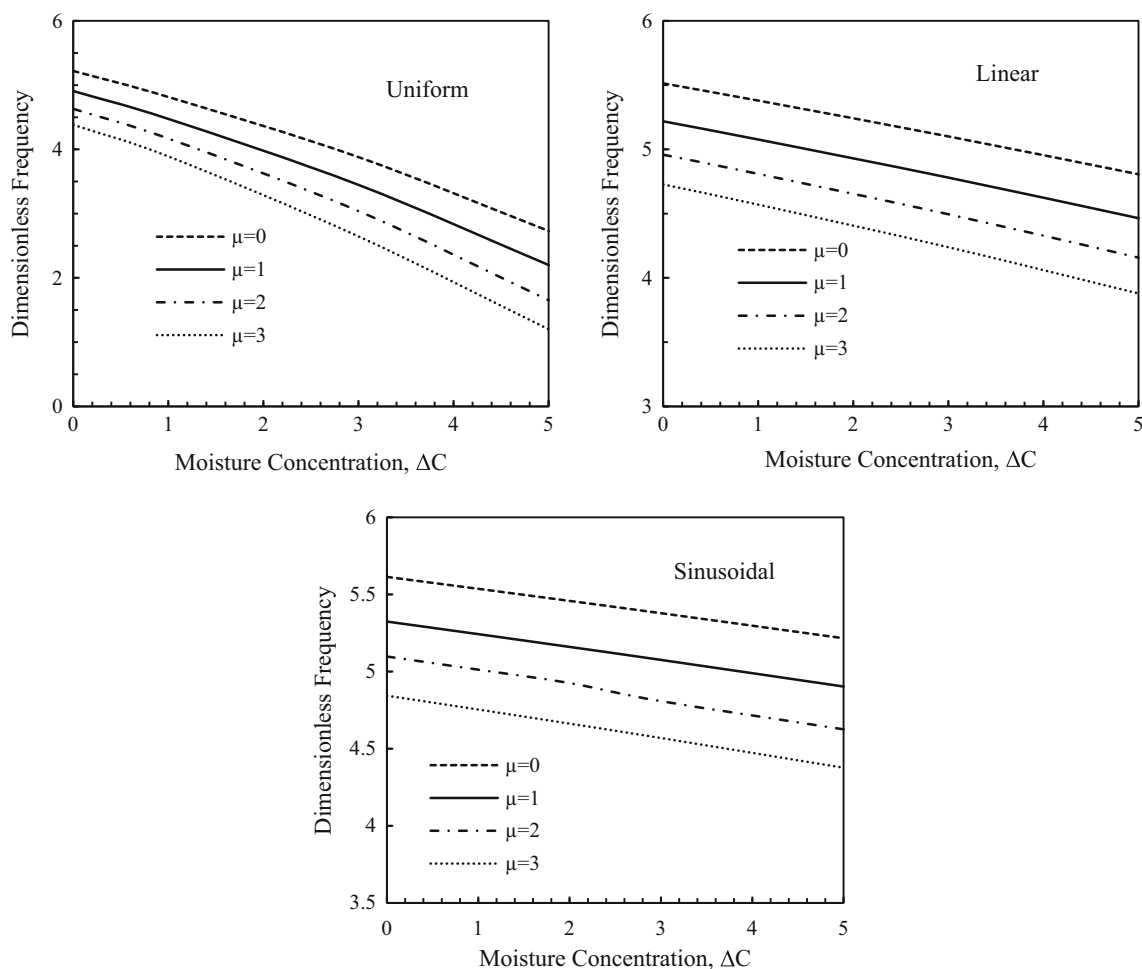


Fig. 2 Influence of moisture and nonlocal parameter on the dimensionless frequency of the S-S FG beam for various hygro-thermal loadings ($p = 1$, $L/h = 20$, $K_w = K_p = 0$, $\Delta T = 40$ (K))

TSDT, HSDT, ESDT, and ITSDT). Material properties of the nonlocal FG beam such as Young’s modulus, Poisson ratio, thermal, and moisture expansion coefficients vary through the thickness direction according to power-law model. Temperature-dependent material properties of nonlocal P-FGM beam which is made from steel (SUS 304) with $\beta_m = 0.0005$ and silicon nitride (Si_3N_4) with $\beta_c = 0$ are given in Table 2. The geometry dimensions of the nanobeam are: L (length) = 10 nm, b (width) = 1 nm, and h (thickness) = varied. It is supposed that the temperature rise in fully metal surface of FG nanobeam to reference temperature T_0 is $T_m - T_0 = 5$ K. For comparison study, numerical results are provided to show the validity of present model in the analysis of nanostructures.

Therefore, natural frequency of presented third-order FG nanobeam under linear temperature rise is compared with those obtained by Ebrahimi and Salari [13] for Timoshenko beam model when nonlocal parameter changes from 0 to 4 nm² in Table 3. It is proved that the present model can evaluate the vibrational behavior of FG nanobeams with

excellent agreement. Also, for better presentation of the results, the following dimensionless quantities are adopted:

$$\hat{\omega} = \omega L^2 \sqrt{\frac{\rho_c A}{E_c I}}, \quad K_w = k_w \frac{L^4}{E_c I}, \quad K_p = k_p \frac{L^2}{E_c I} \quad (40)$$

The variations of the dimensionless frequencies of FG nanobeam resting on elastic foundation for various beam theories and three environmental conditions called uniform, linear, and sinusoidal hygro-thermal loadings at $L/h = 20$ are presented in Tables 4, 5, and 6. It is observed that all of the proposed higher-order beam theories provide approximately same results for free vibration of FG nanobeams, and only some negligible differences exist. Also, it is obvious that frequency results of higher-order theories are lower than classical beam theory due to the reason that CBT is impotent to capture shear deformation effect. For any type of hygro-thermomechanical loading, as nonlocal parameter grows, the dimensionless frequency diminishes. The reason is the lower rigidity of the nanobeam when its size reduces.

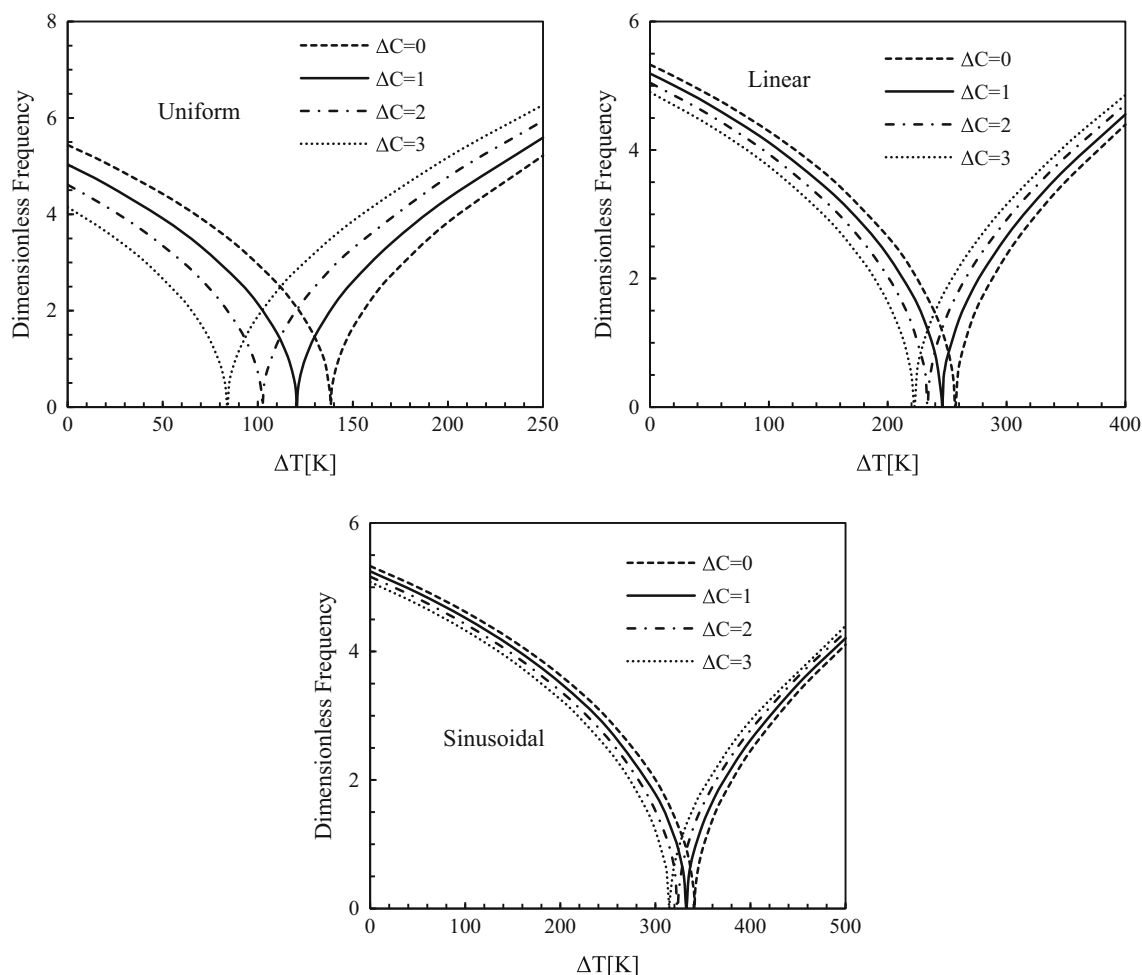


Fig. 3 Influence of moisture concentration on the dimensionless frequency of the S–S FG nanobeam with respect to various temperature rises ($p = 1, L/h = 20, K_w = K_p = 0$)

Also, the rise of moisture and temperature degrades plate stiffness and natural frequencies regardless of hygro-thermal loading type. Therefore, humidity or moisture changes have a notable effect on the mechanical responses of size-dependent FG nanobeams. Moreover, it is found that sinusoidal distribution of temperature and moisture (sinusoidal hygro-thermal loading) provides higher natural frequency than other hygro-thermal loads, while uniform hygro-thermal loading has the lowest one.

The variation of dimensionless natural frequency of simply supported third-order FG nanobeam versus uniform, linear, and sinusoidal moisture concentration rise in pre-buckling domain for different nonlocal parameters at $p = 1$, $L/h = 20$, $K_w = K_p = 0$ and $\Delta T = 40$ (K) is plotted in Fig. 2. At a prescribed humidity condition, the nonlocal beam model estimates lower natural frequency than local beam model. Also, it can be seen that for any type of hygro-thermal loading, the dimensionless frequency degrades with the increase in moisture.

Therefore, moisture concentration and nonlocality have a softening impact on the beam structure and should be considered in the analysis of size-dependent FG nanobeams. Figure 3 shows the dimensionless frequency of S–S higher-order FG nanobeam as function of various temperature rises for different values of moisture concentration at $p = 1$, $L/h = 20$, $K_w = K_p = 0$ and $\mu = 2$ (nm)². It is known that beam structures may buckle with the rise of temperature which creates compressive axial loads. Therefore, for all hygro-thermal loadings with the temperature increment, the natural frequency of FG nanobeam reaches to zero nearby the critical temperature point. This feature refers to stiffness degradation of nanobeam when the temperature grows. After the branching point, the increase in temperature yields larger values of natural frequency. Moreover, it is seen that moisture concentration has a significant impact on the pre-/postbuckling configuration of FG nanobeam under hygro-thermal loads.

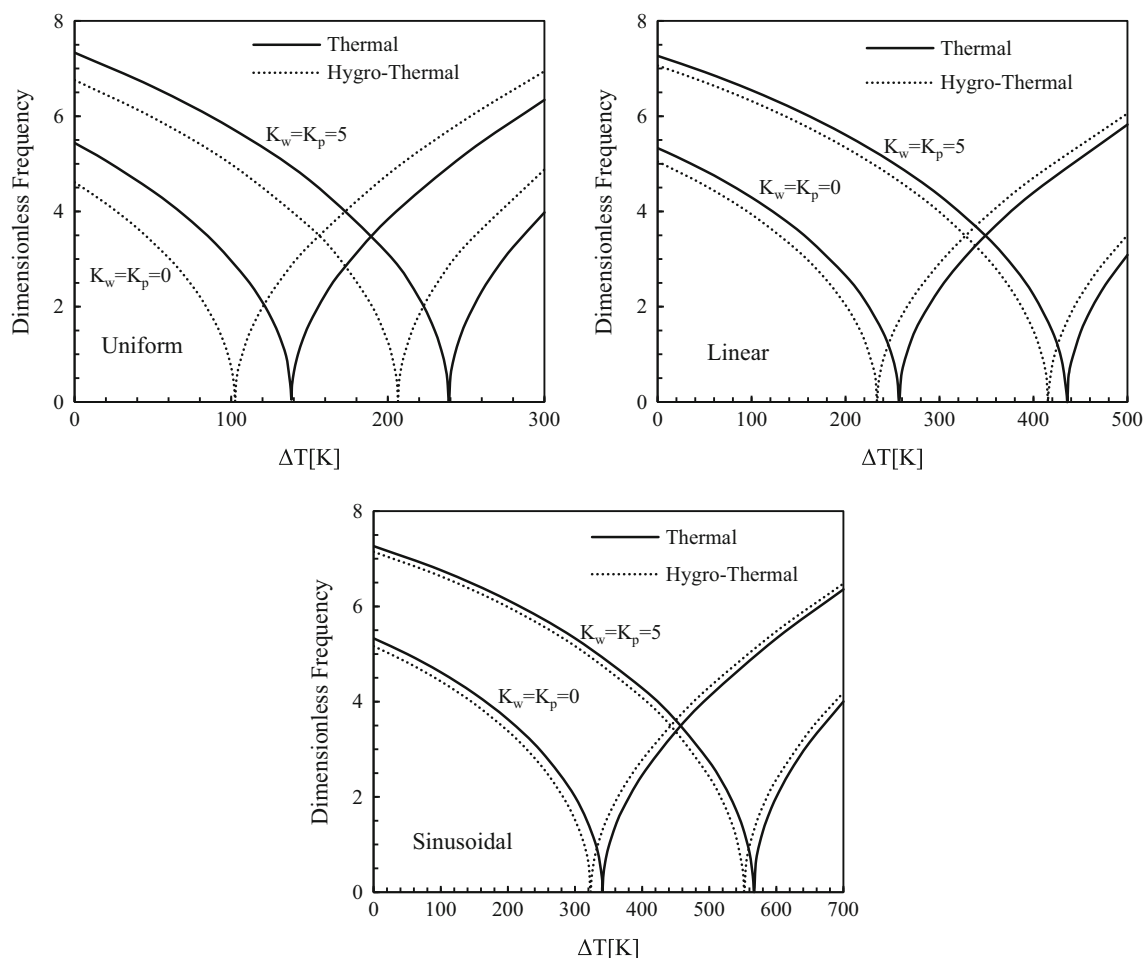


Fig. 4 Influence of elastic foundation on the dimensionless frequency of the S–S FG nanobeam with respect to temperature change for thermal, $\Delta C = 0$ and hygro-thermal, $\Delta C = 2$ environments ($p = 1$, $L/h = 20$, $\mu = 2$ (nm)²)

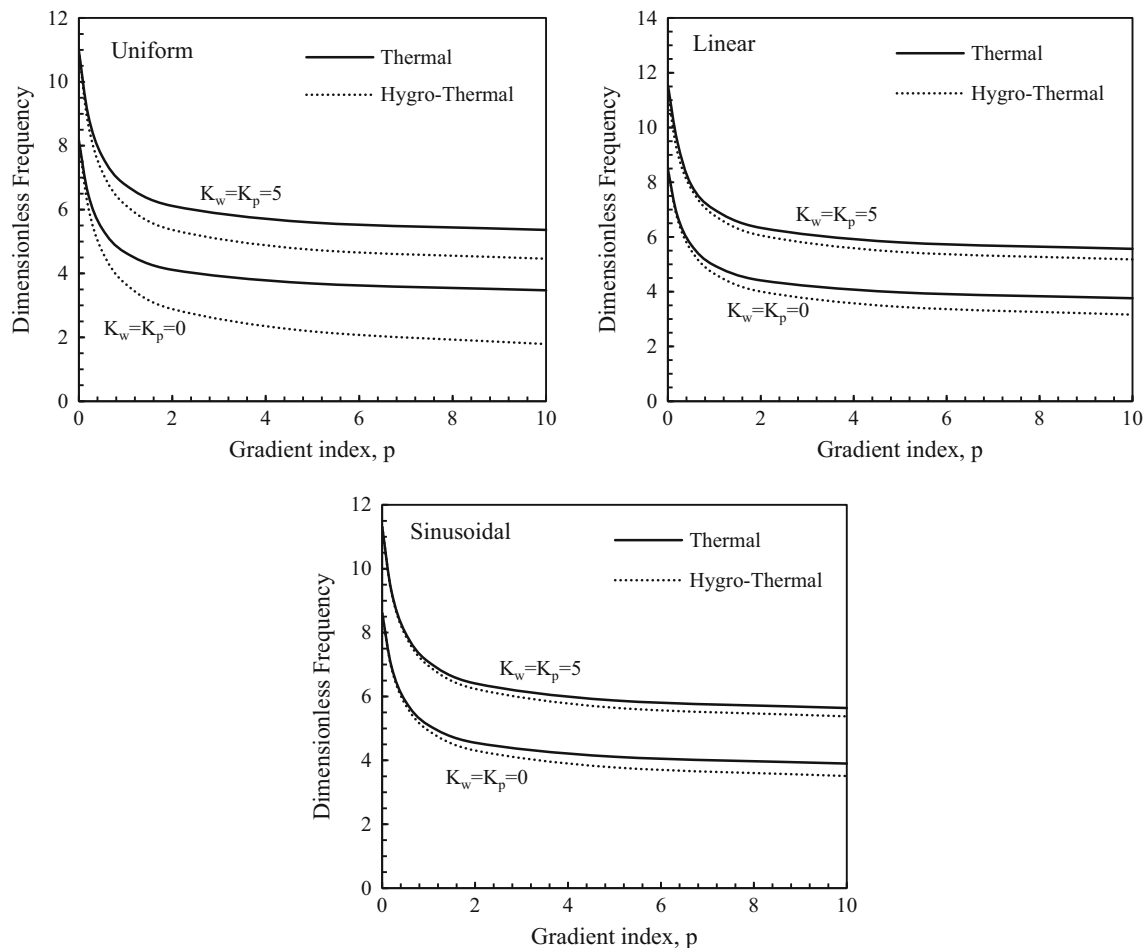


Fig. 5 Influence of material graduation on the dimensionless frequency of the S-S FG nanobeam for thermal, $\Delta C = 0$ and hygro-thermal $\Delta C = 2$ environments ($L/h = 20$, $\mu = 2$ (nm)², $\Delta T = 40$ (K))

Therefore, increasing the value of moisture concentration leads to lower values of the critical buckling temperature, especially in the case of uniform temperature rise. So, imposing a linear or sinusoidal hygro-thermal loading can delay the critical buckling temperature.

Figure 4 indicates the influence of elastic foundation on pre-/post-buckling vibrational behavior of FG nanobeam versus various temperature rises under thermal $\Delta C = 0$ and hygro-thermal $\Delta C = 2$ loadings when $p = 1$, $L/h = 20$ and $\mu = 2$ (nm)². It is found that an increase in Winkler and Pasternak parameters leads to a remarkable postponement in critical buckling temperature. Also, with the presence of moisture or humidity, the critical temperature has shifted to the left which highlights destructive influence of hygroscopic condition on the beam structure.

Figure 5 illustrates the variation of natural frequency with respect to gradient index for various thermal and hygro-thermal loadings with and without elastic foundation at $L/h = 20$ and $\mu = 2$ (nm)². It is observable that under any type of environmental conditions, the natural

frequency reduces with the rise in gradient index, prominently for lower gradient indexes. Moreover, for all values of gradient index, existence of elastic foundation enhances the beam structure and increases the dimensionless frequency. Also, it is found that the effect of moisture concentration on the frequency responses of FG nanobeams is more significant for larger values of gradient index. This is due to the fact that lower values of gradient index are correspond to more portion of the ceramic phase which has a moisture expansion coefficient equal to zero ($\beta_c = 0$).

The influence of slenderness ratio on the natural frequencies of FG nanobeams for various types of thermal and hygro-thermal loadings with and without elastic foundation at $p = 1$ and $\mu = 2$ (nm)² is demonstrated in Fig. 6. For all environmental conditions, the dimensionless frequency increases for lower slenderness ratios and then reduces for higher slenderness ratios which indicates the significance of shear deformation when the beam thickness is large. Also, the influence of moisture concentration on natural frequencies is negligible at lower slenderness ratios so that

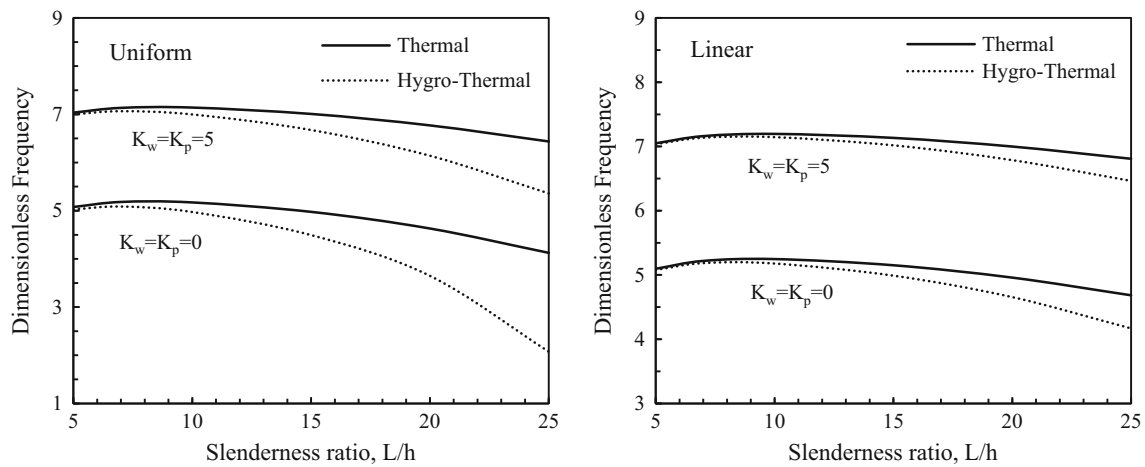


Fig. 6 Influence of slenderness ratio on the dimensionless frequency of the FG nanobeam for various moisture rises ($p = 1, \mu = 2 \text{ (nm)}^2$)

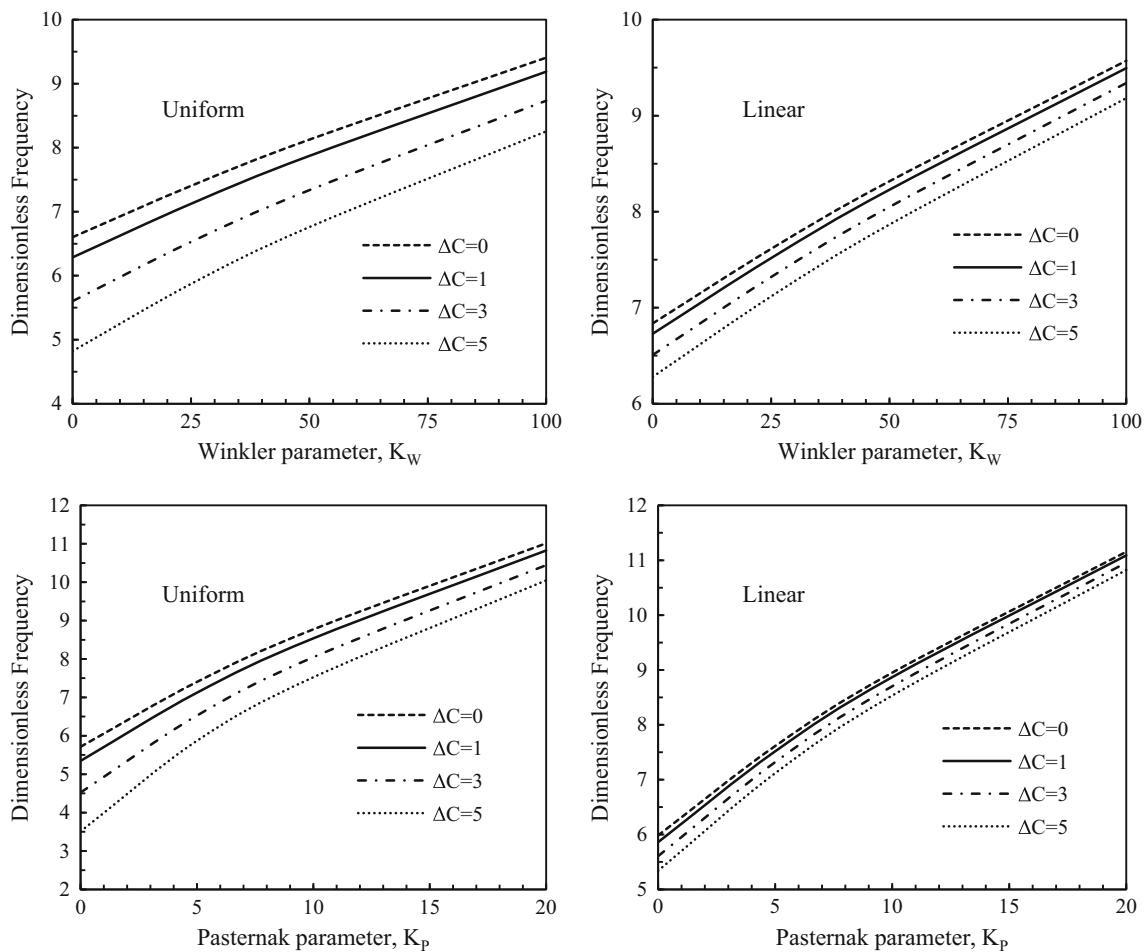


Fig. 7 Influence of elastic foundation parameters on the dimensionless frequency of the FG nanobeam for various moisture rises ($p = 1, \mu = 2 \text{ (nm)}^2, \Delta T = 40 \text{ (K)}$)

it becomes outstanding for larger values of slenderness ratio. So, thinner nanobeams are more affected by the hygro-thermal loadings.

The variation of the dimensionless frequency of S–S higher-order FG nanobeam with respect to Winkler and Pasternak parameters for different uniform and linear

moisture concentrations is presented in Fig. 7, at $p = 1$, $L/h = 20$ and $\mu = 2$ (nm)².

In this figure it is seen that with increase in the Winkler and Pasternak parameters, dimensionless frequency increases for all values of moisture concentration. Also, it is found that the influence of the Pasternak parameter (K_p) on the nondimensional frequency is more prominent than that of the Winkler parameter (K_w). So, it is very important to regard the shear layer of an elastic foundation in the analysis of FG nanostructures.

6 Conclusions

In this paper, hygro-thermomechanical free vibration analysis of embedded functionally graded size-dependent nanobeams exposed to various hygro-thermal loadings is performed by using different higher-order beam theories. Three kinds of environmental conditions namely, uniform, linear, and sinusoidal hygro-thermal loadings are investigated.

Temperature-dependent material properties of nonlocal FG beam change gradually according to the power-law distribution. Size-dependent description of nanobeam is conducted using nonlocal elasticity theory of Eringen. Applying Navier solution the nonlocal coupled governing equations obtained from Hamilton's principle are solved. Finally the impacts of moisture concentration, temperature rise, shear deformation, nonlocal parameter, elastic foundation, material composition, and slenderness ratio on the vibrational characteristics of nanosize FG beams are explored. As a general consequence, all of the higher-order theories provide accurate and approximately same results for the hygro-thermal vibrational behavior of FG nanobeams. The results of higher-order theories are smaller than of classical beam theory since they consider the shear deformation effect. Also, it is seen that the influence of moisture or humidity is significant for higher values of gradient index and slenderness ratio. Moreover, it is found that at a prescribed environmental condition, nonlocality and gradient index have a notable decreasing effect on the natural frequency of FG nanobeams. Also, various hygro-thermal loadings estimate different values of natural frequency and critical temperature so that uniform and sinusoidal hygro-thermal environments produce smallest and largest amount of dimensionless frequency, respectively. Also, it is indicated that with an increase in Winkler or Pasternak parameter, the beam becomes more rigid, and the dimensionless frequency of FG nanobeams enlarges.

References

1. A.H. Akbarzadeh, Z.T. Chen, Hygrothermal stresses in one-dimensional functionally graded piezoelectric media in constant magnetic field. *Compos. Struct.* **97**, 317–331 (2013)
2. Ahouel et al., Size-dependent mechanical behavior of functionally graded trigonometric shear deformable nanobeams including neutral surface position concept. *Steel Compos. Struct.* **20**(5), 963–981 (2016)
3. Ait Amar Meziane et al, An efficient and simple refined theory for buckling and free vibration of exponentially graded sandwich plates under various boundary conditions. *J. Sandwich Struct. Mater.* **16**(3), 293–318 (2014)
4. S.A. Al Khateeb, A.M. Zenkour, A refined four-unknown plate theory for advanced plates resting on elastic foundations in hygrothermal environment. *Compos. Struct.* **111**, 240–248 (2014)
5. E.O. Alzahrani, A.M. Zenkour, M. Sobhy, Small scale effect on hygro-thermo-mechanical bending of nanoplates embedded in an elastic medium. *Compos. Struct.* **105**, 163–172 (2013)
6. Z. Belabed, M.S.A. Houari, A. Tounsi, S.R. Mahmoud, O. Anwar Bég, An efficient and simple higher order shear and normal deformation theory for functionally graded material (FGM) plates. *Compos. Part B* **60**, 274–283 (2014)
7. H. Bellifa, K.H. Benrahou, L. Hadji, M.S.A. Houari, A. Tounsi, Bending and free vibration analysis of functionally graded plates using a simple shear deformation theory and the concept the neutral surface position. *J. Braz. Soc. Mech. Sci. Eng.* **38**, 265–275 (2016)
8. S. Benguediab, A. Tounsi, M. Zidour, A. Semmah, Chirality and scale effects on mechanical buckling properties of zigzag double-walled carbon nanotubes. *Compos. B* **57**, 21–24 (2014)
9. M. Bennoun, M.S.A. Houari, A. Tounsi, A novel five variable refined plate theory for vibration analysis of functionally graded sandwich plates. *Mech. Adv. Mater. Struct.* **23**(4), 423–431 (2016)
10. B. Boudierba, M.S.A. Houari, A. Tounsi, S.R. Mahmoud, Thermal stability of functionally graded sandwich plates using a simple shear deformation theory. *Struct. Eng. Mech.* **58**(3), 397–422 (2016)
11. M. Bourada, A. Kaci, M.S.A. Houari, A. Tounsi, A new simple shear and normal deformations theory for functionally graded beams. *Steel Compos. Struct.* **18**(2), 409–423 (2015)
12. F. Ebrahimi, E. Salari, A semi-analytical method for vibrational and buckling analysis of functionally graded nanobeams considering the physical neutral axis position. *Comput. Model. Eng. Sci. (CMES)* **105**(2), 151–181 (2015)
13. F. Ebrahimi, E. Salari, Effect of various thermal loadings on buckling and vibrational characteristics of nonlocal temperature-dependent FG nanobeams. *Mech. Adv. Mater. Struct.* **23**(12), 1379–1397 (2015)
14. F. Ebrahimi, E. Salari, Thermo-mechanical vibration analysis of nonlocal temperature-dependent FG nanobeams with various boundary conditions. *Compos. B Eng.* **78**, 272–290 (2015)
15. F. Ebrahimi, E. Salari, S.A.H. Hosseini, Thermomechanical vibration behavior of FG nanobeams subjected to linear and non-linear temperature distributions. *J. Therm. Stress.* **38**(12), 1362–1388 (2015)
16. F. Ebrahimi, M.R. Barati, Dynamic modeling of a thermo-piezoelectrically actuated nanosize beam subjected to a magnetic field. *Appl. Phys. A* **122**(4), 1–18 (2016)
17. F. Ebrahimi, M.R. Barati, Vibration analysis of smart piezoelectrically actuated nanobeams subjected to magneto-electrical field in thermal environment. *J. Vib. Control.* (2016). doi:10.1177/1077546316664239

18. F. Ebrahimi, M.R. Barati, Buckling analysis of smart size-dependent higher order magneto-electro-thermo-elastic functionally graded nanosize beams. *J. Mech.* (2016). doi:10.1017/jmech.2016.46
19. F. Ebrahimi, M.R. Barati, Electromechanical buckling behavior of smart piezoelectrically actuated higher-order size-dependent graded nanoscale beams in thermal environment. *Int. J. Smart. Nano Mater.* **7**(2), 69–90 (2016)
20. F. Ebrahimi, M.R. Barati, Small scale effects on hygro-thermo-mechanical vibration of temperature dependent nonhomogeneous nanoscale beams. *Mech. Adv. Mater. Struct.* (2016). doi:10.1080/15376494.2016.1196795
21. F. Ebrahimi, M.R. Barati, A nonlocal higher-order shear deformation beam theory for vibration analysis of size-dependent functionally graded nanobeams. *Arab. J. Sci. Eng.* **41**(5), 1679–1690 (2016)
22. A.C. Eringen, On differential equations of nonlocal elasticity and solutions of screw dislocation and surface waves. *J. Appl. Phys.* **54**(9), 4703–4710 (1983)
23. M.A. Eltaher, S.A. Emam, F.F. Mahmoud, Free vibration analysis of functionally graded size-dependent nanobeams. *Appl. Math. Comput.* **218**(14), 7406–7420 (2012)
24. A. Hamidi, M.S.A. Houari, S.R. Mahmoud, A. Tounsi, A sinusoidal plate theory with 5-unknowns and stretching effect for thermomechanical bending of functionally graded sandwich plates. *Steel Compos. Struct.* **18**(1), 235–253 (2015)
25. H. Hebali, A. Tounsi, M.S.A. Houari, A. Bessaim, E.A. Adda Bedia, A new quasi-3D hyperbolic shear deformation theory for the static and free vibration analysis of functionally graded plates. *ASCE J. Eng. Mech.* **140**, 374–383 (2014)
26. M. Karama, K.S. Afaq, S. Mistou, Mechanical behaviour of laminated composite beam by the new multi-layered laminated composite structures model with transverse shear stress continuity. *Int. J. Solids Struct.* **40**(6), 1525–1546 (2003)
27. F.Z. Kettaf, M.S.A. Houari, M. Benguediab, A. Tounsi, Thermal buckling of functionally graded sandwich plates using a new hyperbolic shear displacement model. *Steel Compos. Struct.* **15**(4), 39 (2013)
28. K. Kulkarni, B.N. Singh, D.K. Maiti, Analytical solution for bending and buckling analysis of functionally graded plates using inverse trigonometric shear deformation theory. *Compos. Struct.* **134**, 147–157 (2015)
29. F. Larbi Chaht, A. Kaci, M.S.A. Houari, A. Tounsi, O. Anwar Bég, S.R. Mahmoud, Bending and buckling analyses of functionally graded material (FGM) size-dependent nanoscale beams including the thickness stretching effect. *Steel Compos. Struct.* **18**(2), 425–442 (2015)
30. C.Y. Lee, J.H. Kim, Hygrothermal postbuckling behavior of functionally graded plates. *Compos. Struct.* **95**, 278–282 (2013)
31. A. Mahi, E.A. Adda Bedia, A. Tounsi, A new hyperbolic shear deformation theory for bending and free vibration analysis of isotropic, functionally graded, sandwich and laminated composite plates. *Appl. Math. Model.* **39**, 2489–2508 (2015)
32. K.S. Na, J.H. Kim, Three-dimensional thermal buckling analysis of functionally graded materials. *Compos. B Eng.* **35**(5), 429–437 (2004)
33. J.N. Reddy, Nonlocal theories for bending, buckling and vibration of beams. *Int. J. Eng. Sci.* **45**(2), 288–307 (2007)
34. M. Sobhy, Hygrothermal vibration of orthotropic double-layered graphene sheets embedded in an elastic medium using the two-variable plate theory. *Appl. Math. Model.* **40**(1), 85–99 (2016)
35. A. Tounsi, M.S.A. Houari, S. Benyoucef, E.A. Adda Bedia, A refined trigonometric shear deformation theory for thermoelastic bending of functionally graded sandwich plates. *Aerosp. Sci. Technol.* **24**, 209–220 (2013)
36. A. Tounsi, S. Benguediab, E.A. Adda Bedia, A. Semmah, M. Zidour, Nonlocal effects on thermal buckling properties of double-walled carbon nanotubes. *Adv. Nano Res.* **1**(1), 1–11 (2013)
37. M. Touratier, An efficient standard plate theory. *Int. J. Eng. Sci.* **29**(8), 901–916 (1991)
38. T.P. Vo, H.T. Thai, T.K. Nguyen, F. Inam, J. Lee, A quasi-3D theory for vibration and buckling of functionally graded sandwich beams. *Compos. Struct.* **119**, 1–12 (2015)
39. J. Peddieson, G.R. Buchanan, R.P. McNitt, Application of non-local continuum models to nanotechnology. *Int. J. Eng. Sci.* **41**(3), 305–312 (2003)
40. A. Zenkour, Hygrothermal analysis of exponentially graded rectangular plates. *J. Mech. Mater. Struct.* **7**(7), 687–700 (2013)
41. A.M. Zenkour, M.N.M. Allam, A.F. Radwan, Effects of transverse shear and normal strains on FG plates resting on elastic foundations under hygro-thermo-mechanical loading. *Int. J. Appl. Mech.* **6**(05), 1450063 (2014)
42. M. Zidi, A. Tounsi, M.S.A. Houari, O.A. Bég, Bending analysis of FGM plates under hygro-thermo-mechanical loading using a four variable refined plate theory. *Aerosp. Sci. Technol.* **34**, 24–34 (2014)